Ground Motions versus Geotechnical and Structural Damage in the February 2011 Christchurch Earthquake

Eleni Smyrou,[1] Panagiota Tasiopoulou,[1] İhsan Engin Bal,[2] and George Gazetas[1]

INTRODUCTION

The $M_w = 6.3$ earthquake of February 22 was the strongest seismic event in a series of damaging aftershocks in and around Christchurch after the Darfield earthquake on 4 September 2010. The source of the Darfield earthquake was in a sparsely populated area and thus it caused no loss of life. Serious damage was mainly due to extensive liquefaction. By contrast, the Christchurch earthquake was generated on a fault in close proximity to the city, resulting in a death toll of 181 people.

The Canterbury Plains are covered with river gravels that hide any evidence of past fault activity in this region. The newly revealed Greendale fault was therefore completely unknown. Only a portion of it was revealed on the ground surface during the Darfield earthquake. The second fault (the one that ruptured in February 2011) appears to be a continuation of the first, although no fault structure directly connecting the faults has been recognized. There is a debate among seismologists at this point whether this is a different fault from Greendale one or not (NHRP 2011a; NHRP 2011b; Geonet 2011).

Due to its magnitude, shallow depth and close proximity to the city, the February earthquake proved particularly destructive for the central business district (CBD) of Christchurch, where buildings suffered extensive damage. Thanks to a dense network of strong ground motion stations, a large number of records have been obtained, which provide valuable information on the event and offer the possibility of relating the extent of damage to actual measurements of ground shaking.

Apart from the southern part of the city on the hills and the Lyttelton port area, Christchurch is built on deep estuarine soil, which has been shaped in the last thousands of years by the ever-changing riverbed. Fine sands—the dominant soil type—and the high ground water level contributed to widespread liquefaction in one or both earthquake events. Often accompanied by lateral spreading, liquefaction amplified the level of damage, resulting in the failure of structures in the CBD and surrounding areas, as will be explained below.

1. Soil Mechanics Laboratory, School of Civil Engineering, National Technical University, Athens, Greece
2. Fyfe Europe S.A. Athens, Greece

The older buildings in the city center, many of which are made of unreinforced masonry with timber floors, were mostly built in the late 19th and early 20th century, following English architectural style and construction practice and with no consideration of the high seismicity of the region. However, some of these buildings had been retrofitted in recent years. In contrast, many of the modern buildings in the CBD were designed in accordance with recent seismic codes, although their foundation systems were not always suitable for the adverse effects stemming from liquefaction. Thus, despite the fact that liquefied layers beneath the CBD restricted somewhat the amplitude of already significantly high accelerations, the increased velocities and displacements due to soil softening magnified the demands on long-period structures. Both structural and geotechnical aspects are investigated here in an effort to broadly explain and quantify the observed damage.

THE STRONG MOTION RECORDS

Thanks to a dense network of seismographs covering the broader area of Christchurch (Figure 1), a large number of ground motions were recorded during the Christchurch February 2011 earthquake. The CBD area includes four seismic stations: CBGS, CCCC, REHS and CHHC. The first three records are truly free-field motions. CHHC was located near the base of a two-story building and its motion may reflect to some degree the effect of the structure. These ground motions may not have been the strongest ones recorded in terms of PGA values; however, due to certain features, their effect on structures or soils was detrimental.

There is a certain variation in the recorded acceleration time histories (Figure 1). For instance, the range of PGA values varies within a factor of 2, from 0.34 g (CHHC-NS) to 0.72 g (REHS-EW). A dominant common feature in all records is the sign of liquefaction: long-period cycles with reduced acceleration amplitudes occurring after a threshold acceleration has been reached. Soil softening due to excess pore water pressures in combination with sufficient acceleration values has led to amplification of large periods affecting a broad category of structures, as indicated by the acceleration spectra. In particular, the spectral

 doi: 10.1785/gssrl.82.6.882

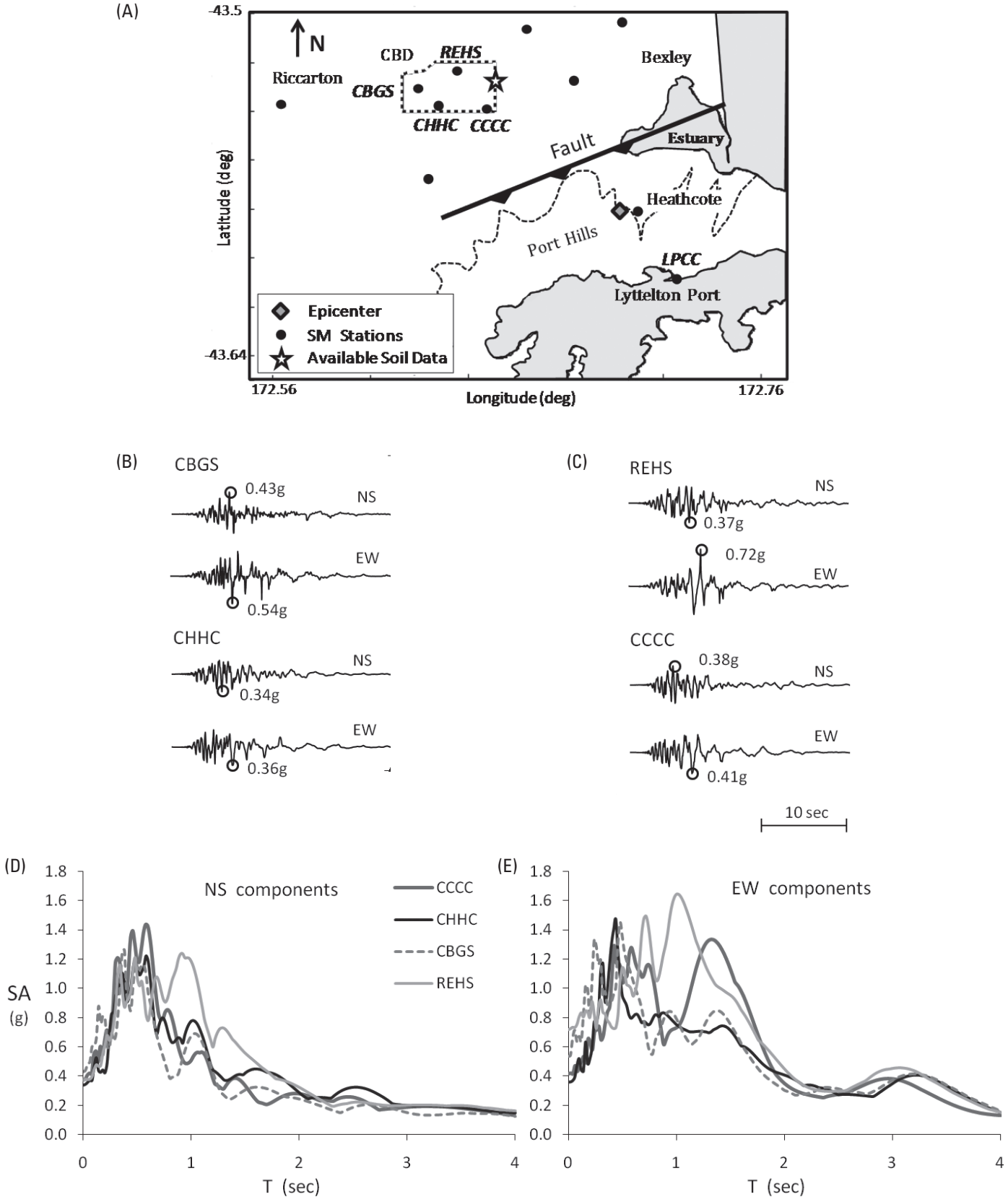

▲ **Figure 1.** A) Map of the broader Christchurch area showing the intersection of the fault plane with the ground surface (from GNS Science), the location of the accelerograph stations, the epicenter of the Christchurch 2011 earthquake, and the location with available soil data. B–E) Acceleration time histories and spectra of four CBD (central business district) seismic stations for NS and EW directions.

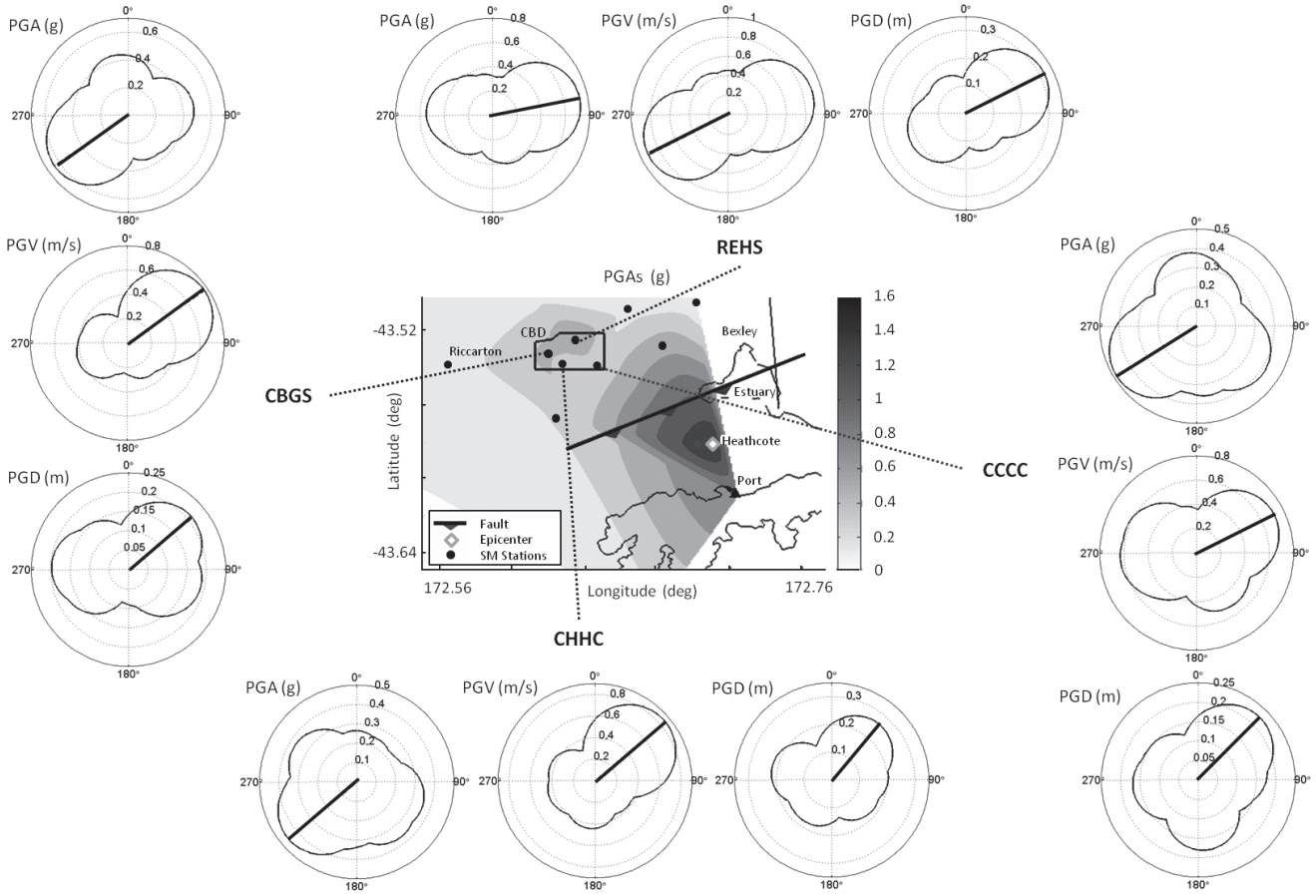

▲ **Figure 2.** Observed polarity for the records in the CBD in terms of peak ground acceleration, velocity, and displacement. The contours of PGA on the map were computed by interpolation using all records in Christchurch.

amplification at periods exceeding 2 sec is attributed to the fact that once liquefaction has occurred, the overlying soil "crust" oscillates with very low frequencies, causing the bulges observed in the acceleration spectra for periods of about 3 sec (see Youd and Carter 2005 for similar observations from the then-available liquefaction-affected acceleration spectra). In addition to structural damage due to high spectral accelerations, important soil-related failures have directly affected houses and bridges.

THE POLARITY OF THE RECORDED MOTIONS

The two orthogonal components of a record are usually aligned with the north-south and east-west directions (Figure 1) or, ideally, if the faults were known, with fault-parallel and fault-normal directions. Mathematically there is at least one specific angle at which a certain ground motion parameter such as PGA, PGV, or PGD reaches a maximum, indicating the governing direction for that ground motion parameter and revealing a certain polarity of the recorded motion. Polarity plots can be useful in determining the dominant shaking direction of an earthquake and in unveiling any directivity effects (Shabestari and Yamazaki 2003).

A first index of intensity is the value of peak ground acceleration (PGA), the spatial distribution of which is depicted on the map of Figure 2. Additionally, for the records from the four CBD stations (CCCC, REHS, CBGS, and CHHC) the *maximum peak values* of ground acceleration, velocity, and displacement are calculated trigonometrically, by varying the angle by 1° between 0° and 180°, resulting in asymmetric plots of positive and negative maxima (in absolute terms). The graphs consistently exhibit distinct polarity in a direction that practically coincides with that of the fault line. Knowing the polarity of shaking may offer information on the rupture mechanism and insight into the dominant damage observed in the CBD area.

TYPICAL SOIL PROFILE, LIQUEFACTION, ANALYSIS

The Christchurch urban area, extending from Riccarton in the west to Bexley in the east and reaching Heathcote Valley and the Port Hills in the south, is located on the Canterbury Plains. Its dominant geomorphic feature is the river floodplains. In particular, the Avon (primarily) and Heathcote (secondarily) rivers, originating from various springs in western Christchurch, form endless meanders through the city and the eastern suburbs as they head to the estuary near the sea.

As depicted in Figure 3A, the subsoil in the CBD systematically consists of profiles with random variations in layering in the upper 15–25 m (Cubrinovski *et al.* 2010; Toshinawa *et al.* 1997). The volcanic bedrock is located at an approximate

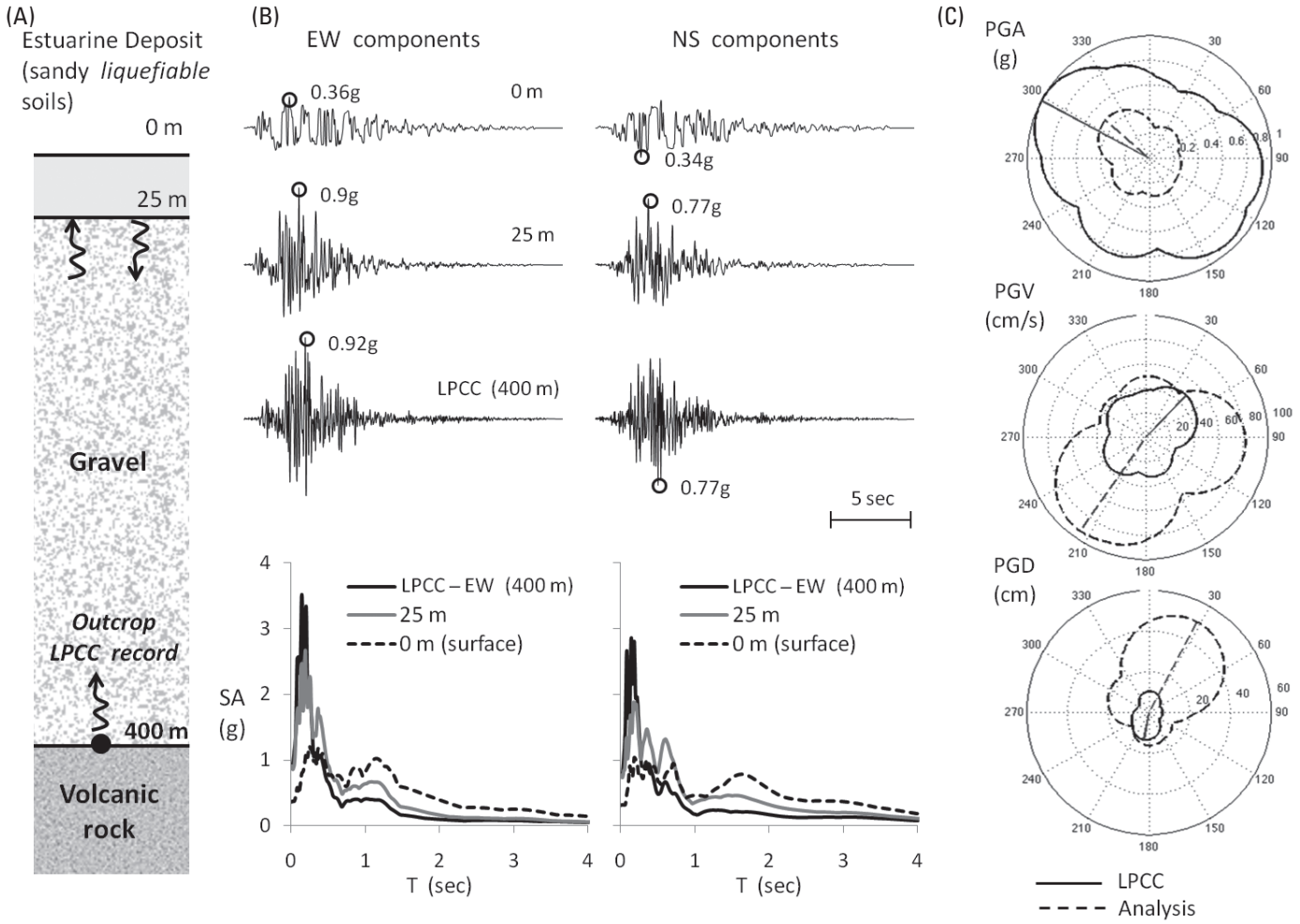

▲ **Figure 3.** A) Typical in-depth soil profile in the CBD. B) Accelerograms and response spectra of the LPCC record used as excitation (applied in outcrop), and at two different depths obtained from the analyses. C) Polarity plots of LPCC record and output of analysis on the ground surface.

depth of 400 m and emerges on the surface at the southern border of the Canterbury Plains, forming the Port Hills of Banks Peninsula. Thick layers of gravel formations overlay the bedrock (Brown and Weeber 1992). The surficial sediments have an average thickness of about 25 m and consist of alternating layers of alluvial sand, silt, and gravel. They have been deposited by overbank flooding (Eidinger *et al.* 2010)—hence, their loose disposition. In the CBD, especially, sand and non-plastic silt with low content of fines are the dominant soil types (Rees 2010). The latter feature combined with the high ground water level (from 0 to 3 m) below the center of the city explains the sensitivity to liquefaction.

There is significant variability of soil deposits within short distances that can differentiate the ground motion characteristics. For example, Toshinawa *et al.* (1997) describe the soil profiles of two characteristic sites 1.2 km distant, one consisting of only sandy gravels and sand close to CBGS seismic station (Figure 1), and the other composed of silt and peat deposits to a depth of 7 m close to REHS seismic station. According to Toshinawa *et al.* (1997), during a 1994 distant earthquake greater amplification was observed at the second site, close to REHS, in agreement with the records of February 2011 (Figure 1). This seems quite reasonable in cases of strong earthquakes, where the response of such soft, mostly sandy soils is expected to be dominated by the effects of severe liquefaction. However, both sites belong to the same broader classification of soft soils (class D) for structural design purposes in the New Zealand design standards (New Zealand Standards 1170.5 2004).

To investigate the soil response in the CBD urban area while accounting for liquefaction effects, we chose a typical "generic" soil profile (Figure 3A). Soil properties were obtained from boreholes conducted close to the Fitzgerald Bridge, situated at the eastern part of the CBD (see the star on the map in Figure 1). Standard penetration test (SPT) values were obtained from Bradley *et al.* (2009) and Rees (2010). Shear wave velocity, V_s, values were based on empirical correlations with SPT (Dikmen 2009).

With the "generic" soil profile defined, dynamic effective-stress analyses were conducted in order to capture the excess pore water pressure rise and dissipation, using the finite difference code FLAC (Itasca Consulting Group 2005). Ground motion recorded at station LPCC on the volcanic outcrop

at Lyttelton Port was selected as the (outcrop) input motion referred to the base of the gravel formations (Figure 3B). The presumption that this rock motion (the only one on [soft] rock in the area) is a suitable candidate for the base of the CBD is only a crude approximation, because although the LPCC and CBD stations have the same distance from the about 65°-dipping fault, LPCC lies on the hanging wall and the CBD on the footwall of this partly thrust and partly strike-slip fault. The NS and EW components of the LPPC record excited the soil column in two different one-dimensional wave propagation analyses. The numerical simulation involves the constitutive law of Byrne (1991) for pore pressure generation, which is incorporated in the standard Mohr-Coulomb plasticity model.

In general, as one would expect, the results of the analysis in terms of acceleration time histories and acceleration spectra for the two components (Figure 3B) demonstrate that as the shear waves propagate from the base of volcanic rock, the soil de-amplifies the low-period components of motion and amplifies those of high period. Moreover, the computed response on top of the dense gravel formation indicates that there is no substantial influence of the gravel layer in altering the input motion, other than de-amplifying the values in the high-frequency range (above 5 Hz) and slightly amplifying lower frequencies. In addition, the peak ground acceleration values do not change.

In contrast to the minor effect of gravel on the soil response, the surficial soil layers play a dominant role in defining the ground motion characteristics—hardly a surprise. These layers behave as a filter cutting off the high frequency spikes, while the duration of motion cycles is lengthened. As a result, the peak accelerations have diminished to 0.35 g approximately in both directions. Moreover, in terms of spectral acceleration values, there is considerable spectral amplification to 1 g in the higher period range of up to 1.8 sec. Overall, both components show similar response, with certain disparities in the frequency content, *e.g.*, N-S output is richer in higher periods.

Polarity plots have also been constructed for LPCC motion and the computed ground surface motion. They are portrayed in Figure 3C. Evidently, there is no single (common) dominant direction for all PGA, PGV, and PGD values, contrary to the consistency in polarity of the CBD records (Figure 2). The PGA principal direction is normal (rather than parallel) to the fault. This discrepancy with CBD polarity might be attributed to the fact that Lyttelton is on the hanging wall side while the CBD lies on the footwall. For the "thrust" component of faulting this difference may indeed have an effect, but this is an issue that needs further investigation and is beyond the scope of this paper. The polarity of the output diverges only slightly from the polarity of LPCC. The comparison of polarity plots demonstrates clearly the cut-off of PGA values in all directions and increase of PGV and PGD values. Evidently, the liquefied layers play the role of a seismic isolator, reducing the acceleration amplitude of the wave components propagating through them.

The occurrence of liquefaction is visible in the pattern of recorded ground acceleration time histories and is captured (with engineering accuracy) in our analysis: pore water pressure increases during shaking, reaching the initial effective overburden stress, σ'_{vo}. At that point onward the soil loses most of its strength and begins to behave as a heavy liquid mass filtering out the high-frequency components, cutting off the acceleration values, and allowing only (long–period) oscillations of the dry cover layer that is "floating" on the top of the liquefied layer.

The ratio of the earthquake-generated (excess) pore water pressure, Δu, normalized by the initial vertical effective overburden stress, σ'_{vo},

$$r_u = \frac{\Delta u}{\sigma'_{vo}},$$

approaches value of 1 at the onset of liquefaction. Values of r_u above 0.8 indicate that already large excess pore water pressures have taken place and the soil has softened significantly. Figures 4B and 4C depict the distribution of computed peak values of $r_u(t)$ with depth and the time histories of $r_u(t)$ at five characteristic depths. In detail, Figure 3B shows that liquefaction did occur from 2.5 m to 17 m ($r_u > 0.8$) throughout the silty sand layer. The dense sand layer experienced some excess pore pressures from flow from the overlying layer, but r_u values were too low for liquefaction, as depicted in the time history of r_u at 18 m (Figure 4C). In addition, according to the time histories of r_u in Figure 4C, liquefaction occurs early, just 3 to 4 sec after the beginning of shaking, which is close to the cut-off of accelerations in the time histories shown in Figure 3B.

To validate the analysis, the authors attempted a comparison between real records and numerical results. The record selected for the comparison, CBGS, is depicted on the map of Figure 1. The CBGS station is located in the Botanic Gardens and the recorder is housed in a very light kiosk (Figure 5A). The signs of liquefaction sand boils are visible, although they had been cleaned following the earthquake (the picture was taken by our research team in April 2011 [Tasiopoulou *et al.* 2011]). No other facilities exist in the surroundings, ensuring free field conditions. Moreover, the soil profile described by Toshinawa *et al.* (1997) is appropriate for this location.

As already discussed, LPCC and the four CBD records have different polarity. However, LPCC was the only option in the search for a rock outcrop motion to be used as excitation in our analysis. That is why the comparison of spectra has been conducted in the direction of polarity of the CBGS record. For example, the strong PGA and PGV direction (polarity) for CBGS is approximately S56W and its PGD polarity is S51W. The acceleration time histories of the CBGS recorded and computed motions in the direction of S56W are depicted in Figure 5B. Although these time histories seem to differ, especially in terms of PGA values, a closer look reveals that they have certain common features, better depicted in Figure 5C after filtering out components with frequency above 4 Hz. Notice in particular that the main pulse at 4 sec exists in both time histories. The response spectral SA, SV, and SD are compared in Figure 5D. The agreement of analysis with reality confirms that the analysis achieves a realistic insight of the mechanisms of soil response during the Christchurch earthquake.

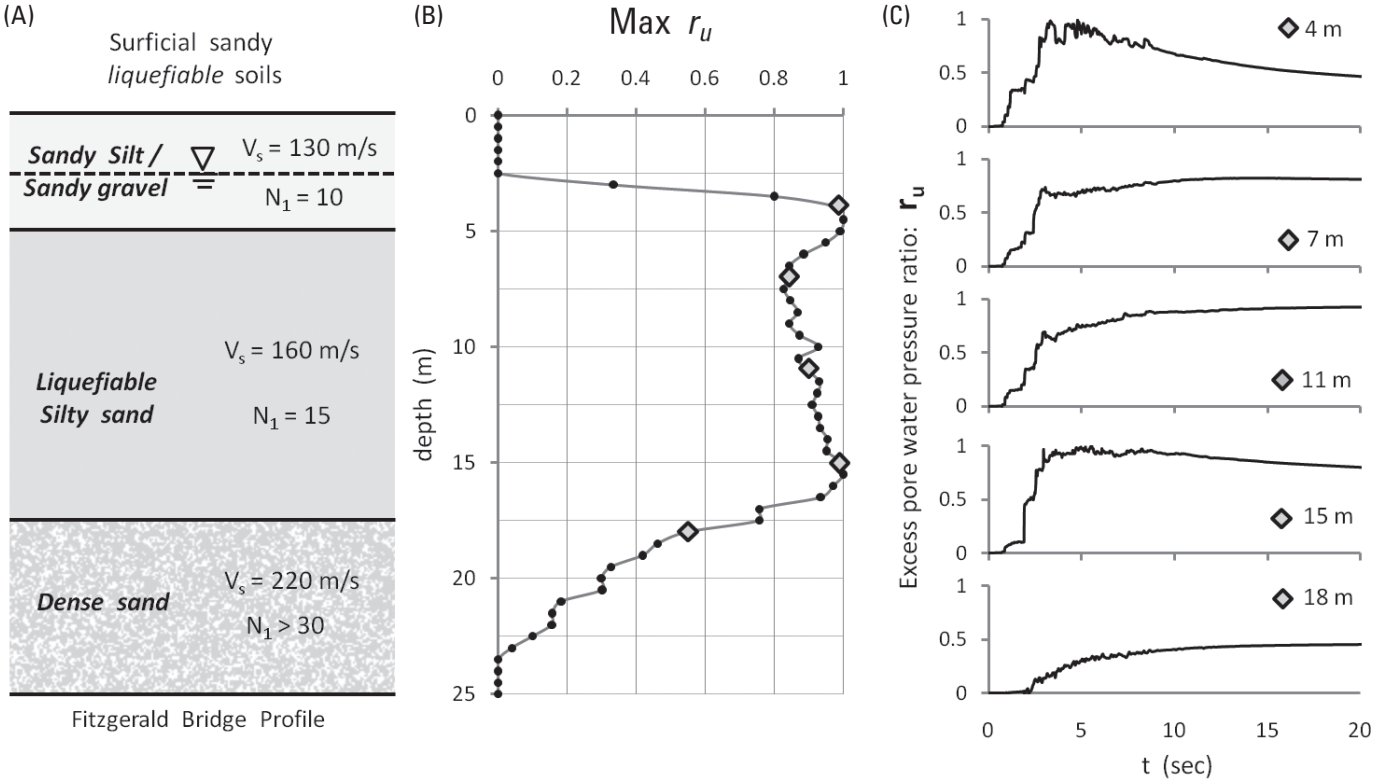

▲ **Figure 4.** A) Typical surficial soil deposit: layers and properties. B) Distribution of computed excess pore water pressure ratio r_u with depth. C) Computed time histories of r_u at several depths.

BUILDING CATEGORIES AND THE OBSERVED DAMAGE

Building Exposure in Christchurch

Structures in New Zealand exhibit great variety. Timber and masonry buildings constitute around 80% of the building stock (Uma *et al.* 2008). Christchurch in particular has many one- or two-story timber and masonry residential buildings outside the CBD and very few modern reinforced concrete (RC) high-rise buildings. The building composition in the CBD is different, with medium-rise modern steel and RC structures as well as mid-rise unreinforced masonry (URM) and timber dwellings and office buildings, some of which date from the late 19th and early 20th centuries. The one-story timber houses are commonly found in the suburbs surrounding the city, especially those along the Avon and Heathcote rivers.

It can be said, roughly, that the area outside the CBD consists of relatively low-rise and light structures, while long-period structures are more abundant in the CBD. This might be one of the reasons for the high concentration of damage in the CBD area during the February 2011 earthquake. A preliminary study presented below investigates the spatial distribution of the drift demands of the recorded strong motions for a range of periods.

Observed Damage

Most of the casualties in the CBD were due to the collapse of two older mid-rise RC structures, called CTV and PGC, the failure conditions of which are presently being investigated. At the time of writing the final statistics regarding the building safety evaluation are not yet available. However, as of 18 March 2011, the data by Civil Defence (Kam et al. 2011) referred to 3,621 buildings checked within the CBD, out of which 1,933 were posted red (needs to be demolished), 862 were posted yellow (has serious damage requiring extensive repair), and 826 were posted green (needs minor repair in order to be usable). More specifically, 19% of the reinforced concrete structures, 14% of the timber, and 7% of the steel buildings checked were evaluated as red, while the equivalent percentages for reinforced and unreinforced masonry structures were 16% and 62%, respectively, reconfirming the poor behavior of URM structures. Insufficient detailing and bad construction techniques, mostly related to non-structural elements, aggravated the damage. Although the aforementioned data have come up before the completion of the second phase of building safety assessment and thus reflect the situation in CBD one month after the earthquake, they offer a representative picture of the extent and severity of damage in the CBD.

Reasons behind the Extended Structural Damage

The demand imposed by the Christchurch earthquake on different structures is assessed in terms of maximum inter-story drift demands (median values of all simulations done for the maximum values of all possible recording directions considered) in an attempt to broadly correlate ground motion features with the spatial distribution of damage. To this end, some characteristic buildings have been selected as representative of

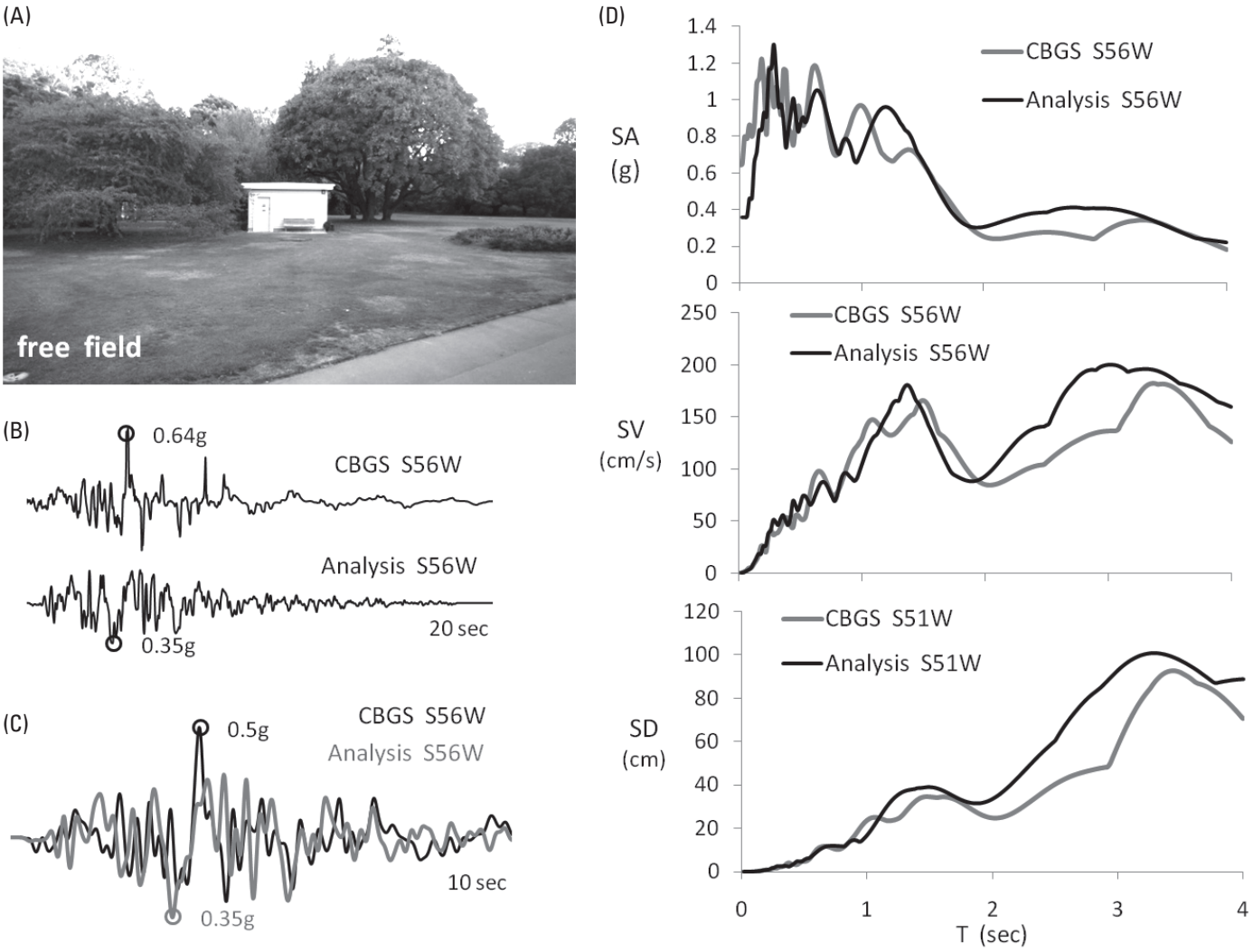

▲ **Figure 5.** A) The CBGS seismic station, with the remnants of liquefaction sand boils seen as scars on the grass. B) Acceleration time histories of CBGS: record and analysis. C) Comparison of the above acceleration time histories after filtering them at 4 Hz. D) Comparison of 5% damped spectra between CBGS record and analysis.

the building stock in the CBD, representing short-, medium-, and long-period structures. Our goal is not, obviously, to study in detail certain structures but to "reconcile" earthquake damage with ground motions. One- and two-story timber residential houses and two RC frame structures of different height, one six stories and one 17 stories, have been examined "generically" as described below in detail. Another case study could select URM buildings, a fairly representative typology in CBD, which suffered much from out-of-plane wall failures.

The selected buildings are treated as reference structures for their category, while the variability in the structural characteristics within each structural category is assumed to follow a statistical distribution simulated through a Monte-Carlo algorithm. This approach is a necessity since at this stage detailed structural data are not available. The parameters of the statistical distribution, *i.e.*, mean value, coefficient of variation, type of distribution, etc., are either taken from the available literature or estimated using engineering judgment guided by the (macroscopic) visual inspection. The assumed values, as well as the relative references for each parameter and structural category examined, are summarized in Table 1.

Having created a large number of simulated buildings, we applied the displacement-based assessment procedure established by Priestley *et al.* (2007) to evaluate the demand on each building. This is then translated to displacement demands for each floor and to inter-story drifts, utilizing the displacement profiles proposed in Priestley *et al.* (2007). The method is based on the substitute-structure theory, first suggested by Gülkan and Sözen (1974) and Shibata and Sözen (1976), according to which an inelastic multi-degree-of-freedom (MDOF) system can be represented by an equivalent inelastic single-degree-of-freedom system (SDOF). The only aspect of our methodology that, out of necessity, deviates from the Priestley *et al.* (2007) is that the "yield period" of each structural category is based on literature suggestions rather than an initial estimate of stiffness and the mass of each specific building. The "yield period" refers to the stiffness at the point of yielding, which is the limit beyond which substantial inelastic response begins that eventually may lead to

TABLE 1
Key Parameters Used in the Representative Analyses

Case Study	Key Parameters	Ranges Used in Monte Carlo Simulations*	Reference for the Key Parameters
1- and 2-story timber	Displacement limit states	μ = 8 mm, CoV = 0.15, [N]	Uma *et al.* 2008
	Equivalent viscous damping equation	Deterministic	NZSEE 2006
	Ratio of the first yield to the base shear coefficient	a = 0.5, b = 0.8, [U]	ATC 1996
	Story height	a = 2.8 m, b = 3.1 m, [U]	Field data
6-story RC frame	Beam depth	μ = 0.8 m, CoV = 0.15, [N]	Tasiopoulou *et al.* 2011
	Beam length	μ = 7.0 m, CoV = 0.15, [N]	Tasiopoulou *et al.* 2011
	Rebar yield strength	μ = 330 MPa, CoV = 0.15, [N]	Uma *et al.* 2008
	Yield-period equation	Deterministic	Crowley *et al.* 2004
	Equivalent viscous damping equation	Deterministic	Priestley *et al.* 2007
17-story RC frame	Beam depth	μ = 0.6 m, CoV = 0.15, [N]	Galloway *et al.* 2011
	Beam length	μ = 5.0 m, CoV = 0.15, [N]	Galloway *et al.* 2011
	Rebar yield strength	μ = 330 MPa, CoV = 0.15, [N]	Uma *et al.* 2008
	Yield-period equation	Deterministic	Crowley *et al.* 2004
	Equivalent viscous damping equation	Deterministic	Priestley *et al.* 2007

* μ: mean, CoV: coefficient of variation, [N]: Normal distribution, [U]: Uniform distribution, a and b: limits of the uniform distribution.

significant damage. The yield period has been successfully used as a key parameter in performance assessment by Crowley *et al.* (2004) and Bal *et al.* (2010). References for the parameters used for each category of buildings are given in Table 1.

To ensure that the maximum displacement demand is estimated, the components for each record have been rotated in increments of 1° degree from 0° to 180°, thus creating a new set of 180 records and the corresponding response spectra. The contours of the maps presented in the paper (see Figures 6 to 8) have been derived after assessing each simulated building for a total of 180 response spectra. Note that the inter-story drift demands have been calculated only at the position of the recording stations, as shown on the maps in Figures 6 to 8. The values presented between the stations are only the result of linear interpolation among several "anchor" points. Obviously, the interpolation in these figures is bound by the coastline and cannot be extended to Kaiapoi and to Lyttelton Port stations.

Short-period structures are mostly timber buildings. Such two-story houses are found in the CBD, while one-story houses are outside the CBD and in the suburbs. They are non-engineered buildings, with few if any exceptions; local regulations allow simple timber houses to be constructed without an approved design. Both groups were significantly damaged, but only a few collapsed. However, the damage to such houses due to liquefaction-induced ground differential settlements and horizontal displacements was unprecedented. A generic building has been used in this study as a reference structure. The properties of this generic structure are taken from the work by Uma *et al.* (2008), in which the story drift limits are given as 0.3%, 0.6%, 1.2%, and 1.6% for slight, moderate, significant damage, and collapse limit states. Details of the assumed parameters can be found in Table 1.

There are several commercial buildings in the CBD, most of which are mid-rise RC structures designed and built in the 1970s and 1980s when the developed modern design concepts had only partially (at best) been incorporated in codes. A specific building from Kilmore Street (Markham's Building), shown in Figure 9, is used for generating an ensemble of similar buildings for moderately long-period structures. Despite widespread liquefaction in the area, its pile foundation helped to limit the damage; thus, the results presented below refer to similar buildings founded on stable upper soil layers. The final case study is a real building in Worchester Street, known as Clarendon Tower, which has been reported to have undergone significant but repairable damage in the February earthquake. It is a regular moment-resisting frame structure, the details of which are given in Galloway *et al.* (2011).

The spatial distribution of the mean values of inter-story drift demands in Christchurch for two-story timber structures (Figure 6), computed using the approach described above, clearly suggests that there must have been concentration of the inter-story demand in and near the Heathcote Valley where the strongest recorded shaking (HVSC) in terms of PGA and low-period SA and SD took place. On the contrary, damage in the area of the CBD must have been somewhat lighter, apparently due to the smaller low-period SD in the CBD. Such differences can be attributed to the somewhat larger distance from the source and the fact that the soft soils de-amplified the short-period seismic waves. But still, the median inter-story drift demands in the CBD are computed to have been in the order of 1.0%–1.5% for two-story timber structures, a level of demand definitely sufficient to induce substantial structural damage. Indeed, observations from different parts of the CBD on a variety of timber two-story structures confirm this theo-

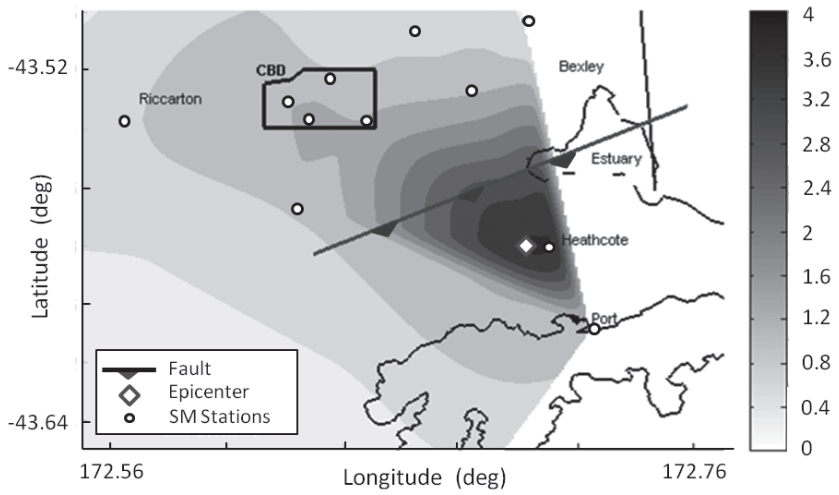

▲ **Figure 6.** Computed median inter-story drift demands (%) on two-story timber structures:maximum of all possible recording directions is considered (coefficient of variation of the results: 31%).

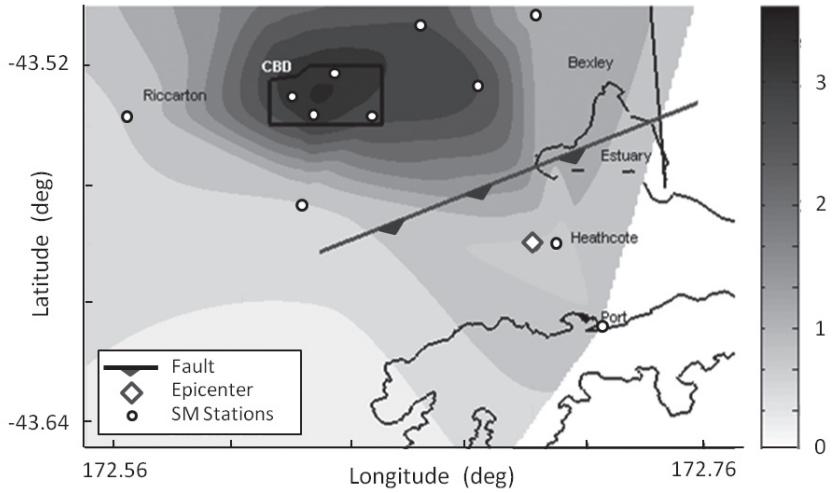

▲ **Figure 7.** Computed median inter-story drift demands (%) on six-story RC frame structures:maximum of all possible recording directions is considered (coefficient of variation of the results: 19%).

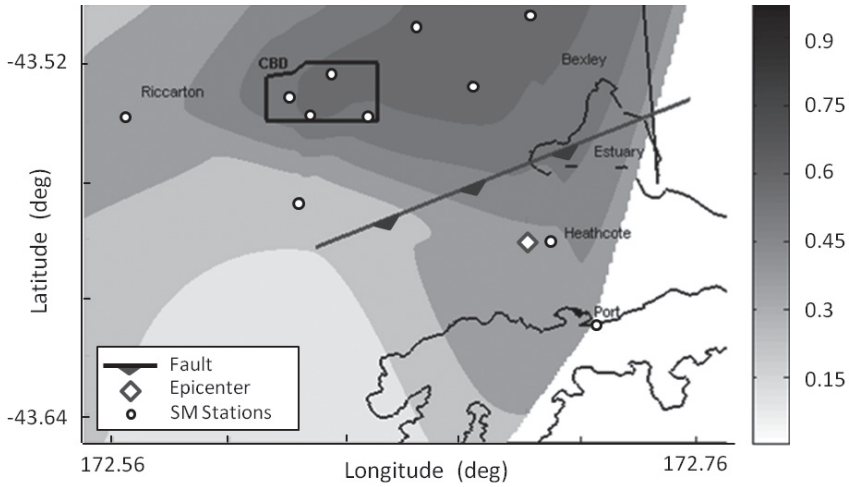

▲ **Figure 8.** Computed median inter-story drift demands (%) on 17-story RC frame structures:maximum of all possible recording directions is considered (coefficient of variation of the results: 19%).

▲ **Figure 9.** Representative buildings for the considered categories: timber residential house (left), mid-rise RC structure (middle), and tall RC structure (right).

retical finding. Analyses on one-story timber structures with similar assumptions showed that the expected drift demands were quite limited, thus explaining the low damage ratio of one-story houses.

The computed spatial distribution of the median inter-story drift demands for six-story RC frames is portrayed in Figure 7, which shows that the highest demands on such structures, in the order of 3.0–3.5% inter-story drifts, are concentrated in the CBD—which explains the damage on mid-rise RC structures during the February 22 earthquake. Interestingly, the computed damage potential for such structures specifically reaches its climax in the CBD. Readers are reminded that both the CTV and PGC buildings, which fatally collapsed from the February shaking, were mid-rise RC structures constructed on soft soil.

Tall RC frame structures in the CBD, though limited in number, also experienced some extent of damage with the most characteristic case being that of the Grand Chancellor Hotel, a 26-story wall-frame structure that was rendered unusable due to large residual displacement. The building we chose to look at, the Clarendon Tower, underwent significant but repairable damage. Nevertheless, the building will be demolished as not meeting insurance standards. The findings illustrated in Figure 8 exhibit 0.6% to 0.8% median inter-story drift demands for similar 17-story structures, a drift level that certainly translates into damage but remains below the unrepairable drift limits in line with field observations (Tasiopoulou *et al.* 2011).

The inter-story drift demands reach their peak in the CBD as shown in Figure 8, a fact that could arguably be attributed to the characteristic bulges appearing in the response spectra (Figure 1) in the range of long periods. The elastic fundamental period of such structures is estimated around 2 sec, while the yield period (beyond which significant damage arises), is of the order of 5 sec (Crowley *et al.* 2004). The effective secant period, for example, is expected to elongate up to about 7 sec in the case of an overall ductility equal to 2, as computed with the approximate expression for effective period of Priestley and Kowalsky (2000).

CONCLUSIONS

Damaging earthquakes feature large variations in spatial distribution of the strong ground motion parameters, a fact that is mostly attributed to the complexity of source mechanism, radiation pattern, and site conditions. The $M_w = 6.3$ Christchurch earthquake was a surprising and unusual event which occurred in an unknown fault that had already been awakened by the September 2010 stronger earthquake, and it had a strong thrust component and a steeply dipping plane.

This paper has attempted to identify quantifiable parameters that could provide better insight to seismologists and engineers who try to systematically investigate the reasons behind the structural and soil failures that occurred in the February shaking. The study focuses on connecting the basic features of the recorded strong motions to the nonlinear behavior of the soil layers. Liquefaction, a phenomenon that played a major and devastating role, has been examined through a "generic" downtown soil profile and dynamic effective stress analysis. The LPCC record was applied as the base excitation, as it was the only available rock outcrop motion. Despite several uncertainties, the output spectra obtained from the liquefaction analyses and the one recorded in the free field in the Botanic Gardens have shown quite a satisfactory match provided that the compared spectra are aligned with the strong direction of the recorded motion. The dominant direction of the CBGS record is consistently almost parallel to the fault plane while the Lyttelton record exhibits more inconsistencies, something that may be related to the effects of the hanging wall and the steep thrust-fault plane. The governing direction of each record has been found by simply turning the record in every possible direction with one-degree intervals and re-recording the strong motion parameters sought—a venerable procedure to uncover the dominant direction of the shaking of a given site.

The paper concludes with an effort to better explain the reasons why some particular structural types showed bad performance in the CBD area. Short, medium, and long period

structures have been examined adopting a displacement-based procedure. Results show that the inter-story drift demands in the CBD were particularly damaging for all types of structures but especially catastrophic for mid-rise RC buildings on shallow foundations. This is an important finding that may contribute to understanding why the CTV and PGC buildings collapsed.

ACKNOWLEDGMENTS

Financial support for the expedition to the earthquake-stricken area and the work outlined in this paper has been provided under the research project "DARE," funded through the "IDEAS" Programme of the European Research Council (ERC) under contract number ERC-2-9-AdG228254-DARE. The authors would like to thank Professors John Berrill, Misko Cubrinovski, Stefano Pampanin, and Dr. Umut Akgüzel for providing data and assisting the authors during their reconnaissance visit in Christchurch in April 2011.

REFERENCES

Applied Technology Council (ATC) (1996). *Seismic Evaluation and Retrofit of Concrete Buildings*. ATC-40 Report, vols. 1 and 2. Redwood City, CA: Applied Technology Council.

Bal, İ. E., J. J. Bommer, P. J. Stafford, H. Crowley, and R. Pinho (2010). The Influence of Geographical Resolution of Urban Exposure Data in an Earthquake Loss Model for Istanbul, *Earthquake Spectra* **26** (3), 619–634.

Bradley, B. A., M. Cubrinovski, R. P. Dhakal, and G. A. MacRae (2009). Probabilistic seismic performance assessment of a bridge-foundation-soil system. *Soil Dynamics and Earthquake Engineering* **30**, 395–411.

Brown L. J., and J. H. Weeber (1992). *Geology of the Christchurch Urban Area*. Institute of Geological and Nuclear Sciences, Scale 1:25,000, Geological Map 1, New Zealand. Lower Hutt, New Zealand: GNS Science.

Byrne, P. (1991). A cyclic shear-volume coupling and pore-pressure model for sand. *Proceedings of the Second International Conference on Recent Advances in Geotechnical Earthquake Engineering and Soil Dynamics, St. Louis, Missouri*, 47–55.

Crowley, H., and R. Pinho (2004). Period-height relationship for existing European reinforced concrete buildings. *Journal of Earthquake Engineering* **8** (S1), 305–332.

Cubrinovski, M., R. Green, J. Allen, S. Ashford, E. Bowman, B. Bradley, B. Cox, T. Hutchinson, E. Kavazanjian, R. Orense, M. Pender, M. Quigley, T. Wilson, and L. Wotherspoon (2010). Geotechnical reconnaissance of the 2010 Darfield (New Zealand) earthquake. *Bulletin of the New Zealand Society for Earthquake Engineering* **43**, 243–320.

Dikmen, Ü. (2009). Statistical correlations of shear wave velocity and penetration resistance for soils. *Journal of Geophysics and Engineering* **6**, 61–72.

Eidinger, J., A. Tang, and Thomas O'Rourke (2010). *Technical Council on Lifeline Earthquake Engineering (TCLEE), Report of the 4 September 2010 Mw 7.1 Canterbury (Darfield), New Zealand Earthquake*. Reston, VA: American Society of Civil Engineers.

Galloway, B. D., H. J. Hare, and D. K. Bull (2011). Performance of multi-storey reinforced concrete buildings in the Darfield earthquake. *Proceedings of the Ninth Pacific Conference on Earthquake Engineering—Building an Earthquake-Resilient Society, 14–16 April, 2011, Auckland, New Zealand*, paper no. 168.

Geonet (2011). Christchurch badly damaged by magnitude 6.3 earthquake (22 February 2011), http://www.geonet.org.nz.

Gülkan, P., and M. Sözen (1974). Inelastic response of reinforced concrete structures to earthquake motions. *ACI Journal* **71** (12), 604–610.

Itasca Consulting Group (2005). *Fast Lagrangian Analysis of Continua*. Minneapolis, MN: Itasca Consulting Group Inc.

Kam, W. Y., U. Akguzel, and S. Pampanin (2011). *4 Weeks on: Preliminary Reconnaissance Report from the Christchurch 22 Feb 2011 6.3M_w Earthquake*. Report, New Zealand Society for Earthquake Engineering Library, Wellington, New Zealand.

Natural Hazards Research Platform (NHRP) (2011a). Why the 2011 Christchurch earthquake is considered an aftershock, http://www.naturalhazards.org.nz.

Natural Hazards Research Platform (NHRP) (2011b). Magnitude 6.3 earthquake not on Greendale Fault, http://www.naturalhazards.org.nz.

New Zealand Society for Earthquake Engineering (NZSEE) (2006). *Assessment and Improvement of the Structural Performance of Buildings in Earthquakes*, New Zealand Society for Earthquake Engineering.

New Zealand Standards 1170.5 (2004). *Structural Design Actions, Part 5: Earthquake Actions—New Zealand*. Wellington, New Zealand: Standards New Zealand, 82 pp.

Priestley, M. J. N., G. M. Calvi, and M. J. Kowalsky (2007). *Displacement-based Seismic Design of Structures*. Pavia, Italy: IUSS Press.

Priestley, M. J. N., and M. J. Kowalsky (2000). Direct displacement-based seismic design of concrete buildings. *Bulletin of the New Zealand National Society for Earthquake Engineering* **33** (4), 421–444.

Rees, S. D. (2010). Effects of fines on the un-drained behavior of Christchurch sandy soils. PhD thesis, Civil and Natural Resources Engineering, University of Canterbury, Christchurch, New Zealand.

Shabestari, K. T., and F. Yamazaki (2003). Near-fault spatial variation in strong ground motion due to rupture directivity and hanging wall effects from the Chi-Chi, Taiwan earthquake. *Earthquake Engineering and Structural Dynamics* **32**, 2,197–2,219.

Shibata, A., and M. Sözen (1976). Substitute structure method for seismic design in reinforced concrete. *ASCE Journal of the Structural Division* **102** (ST1), 1–8.

Tasiopoulou, P., E. Smyrou, İ. E. Bal, G. Gazetas, and E. Vintzileou (2011). *Geotechnical and Structural Field Observations from Christchurch, New Zealand, Earthquakes*. Research Report, National Technical University of Athens, Greece.

Toshinawa, T., J. J. Taber, and J. B. Berrill (1997). Distribution of ground-motion intensity inferred from questionnaire survey, earthquake recordings, and microtremor measurements: A case study in Christchurch, New Zealand, during the 1994 Arthurs Pass earthquake. *Bulletin of the Seismological Society of America* **87**, 356–369.

Uma, S. R., J. Bothara, R. Jury, and A. King (2008). Performance assessment of existing buildings in New Zealand. *Proceedings of the New Zealand Society for Earthquake Engineering Conference, Wairakei, New Zealand, 11–13 April*, paper no. 45.

Youd, T. L., and B. L. Carter (2005). Influence on soil softening and liquefaction on spectral acceleration. *ASCE Journal of Geotechnical and Geoenvironmental Engineering* **131** (7), 811–825.

Soil Mechanics Laboratory
School of Civil Engineering
National Technical University
Heroon Polytechneiou 9
Zografou Campus
Athens 15780 Greece
smiroulena@gmail.com
(E. S.)